A meso-mechanical model of the tensile behaviour of concrete. Part I: modelling of the pre-peak stress–strain relation

J. HUANG and V. C. LI

(Massachusetts Institute of Technology, USA)

A constitutive model is derived for the pre-peak non-linear stress–strain relation for concrete based on analysis of the internal structure and local deformation mechanisms. Inelastic deformation is accounted for by considering the opening of stably propagating interfacial cracks at cement matrix/aggregate interfaces. Analytical expressions for inelastic deformation and composite tensile strength are derived as functions of maximum aggregate size, aggregate volume fraction and cement matrix toughness. Limited comparisons between model predictions and experimental data are presented.

Key words: *concrete; tension; stress–strain relation; inelastic deformation; tensile strength; maximum aggregate size; aggregate volume fraction*

Concrete is a very brittle material with low tensile load bearing capacity. Compared to structural steel, concrete has only 0.1 to 1% of its tensile strength, and only 0.2 to 4% of its fracture toughness. For this reason, while concrete structures are often reinforced and/or pre-stressed, tensile failure can often occur. Tensile failures have been observed under compressive, shear, flexural and torsional ambient loading, especially when the concrete is lightly confined.

The internal structure of concrete is made up of cement paste, fine aggregate, large or coarse aggregates and voids in the paste. Although cracking may start from voids in the paste, it is generally accepted that in normal concrete, the cement/aggregate interface provides a weak link which limits the strength of the material. This is because of the existence of bond cracks caused by bleeding, usually on the lower side of the aggregate in concrete placements.[1] In addition, Slate and Matheus[2] found that cement shrinkage during setting and hardening can induce bond cracks. In normal concrete, the bond strength is only 33 to 67% of the mortar tensile strength.[3] These bond cracks provide natural flaw sites to initiate interfacial cracks which may subsequently branch into the cement matrix; observations of interfacial cracks have been made by many researchers.[1,4] Although bond cracks can limit the strength of the material, they can also provide mechanisms of crack deflection, arrest, blunting and branching when matrix cracks run into the interface between cement and coarse aggregates.[1] This is reflected in the tortuosity of the fracture plane in concrete resulting in a toughness higher than that of pure cement. These notions suggest that the aggregate volume fractions and size, and the aggregate/cement interfacial strength must contribute significantly to the material tensile properties.

The present paper is a preliminary effort in relating analytically the internal structure and mechanisms of concrete to its macroscopic tensile behaviour. In particular, the model assumes that the nucleation and propagation of interfacial cracks from flaw sites at cement/aggregate interfaces is responsible for the reduced material stiffness and non-linearity after the limit of proportionality is reached in a concrete stress–strain curve. The concrete strength is assumed to be associated with the branching of the most critical interfacial crack into the matrix. The post-peak tension-softening behaviour is related to the propagation of this crack and its interaction with other

0010-4361/89/040361-09 $3.00

interfacial cracks and aggregates. The analysis on the internal material structural scale is based on linear–elastic fracture mechanics and a probabilistic description of aggregate size and interfacial cracks. The paper consists of two parts. In part I, the modelling of the pre-peak stress–strain relation is presented, followed by part II, the modelling of post-peak tension-softening behaviour. Important internal material parameters are identified and their effects on tensile behaviour discussed. Model predictions based on typical ranges of such internal material parameters are compared to available experimental data.

Previous modelling of the stress–strain relation

The pre-peak stress–strain relation of concrete in tension has been studied by many researchers.[5–16] The theoretical modelling of the stress–strain relation in tension is approached using different methods. Lorrain and Loland[11] and Mazars[12] studied the progressive deterioration of concrete under monotonic or repeated loading based on damage mechanics. Based on the weakest link concept originated by Weibull,[17] and by assuming a probability density function of flaws, Mihashi[13] and Hu *et al*[14] related the probability of failure to a given stress level for a brittle material. Zielinski[10] studied the tensile behaviour of concrete by considering the processes of crack initiation and growth in connection with the state of stress in concrete with inherent microcracks, focusing especially upon effects associated with high rates of loading. In addition, Ortiz[15] established constitutive relations for cement paste and aggregate, and then predicted the composite nature of concrete by means of mixture theory. Finally, Zaitsev[18,19] and Hu *et al*[16] began investigating the formation and extension of a single crack, either at the cement/aggregate interface or within the cement matrix, and then using computer simulation to model the behaviour of concrete with randomly distributed aggregates.

These works generally recognize the brittle nature of concrete and include some form of fracture mechanics in the model. The random nature of material defects are also taken into account either analytically or numerically. Some of the models have quite successfully simulated concrete behaviour under various loading conditions (static, dynamic, fatigue, *etc*) and even environmental conditions (*eg* temperature). Apart from Refs 16, 18 and 10, however, most models do not explicitly relate the internal material structures and mechanisms of deformation to the macroscopic properties. Such connections are necessary for the purpose of engineering the internal structure for desirable material properties.

BASIC ASSUMPTIONS OF THE MODEL

As in Refs 18, 22 and 25, the aggregates are modelled as circular discs with a random size distribution. In the analysis of the pre-peak stress–strain relation, two assumptions are made. First, for normal concrete, the magnitudes of toughness are assumed to be

$$K_{Ic}^{if} < K_{Ic}^{m} < K_{Ic}^{agg} \qquad (1)$$

where K_{Ic}^{if} is the interface toughness, K_{Ic}^{m} is the cement matrix toughness, and K_{Ic}^{agg} is the aggregate toughness. This assumption is supported by experimental studies[23,24] on normal concrete. It is also consistent with observations[20–22] that cracking in mortar or concrete begins in the cement/aggregate interfacial region and that crack paths generally run through interfacial zones.

The second assumption concerns the neglecting of mechanical interaction between aggregates. In this preliminary study, these interactions are neglected. The assumption can be justified only if the aggregate volume fraction is small (which unfortunately is usually not the case in real concrete). (These issues will be addressed in a further investigation). The effect of the interaction between interfacial cracks on the tensile strength is accounted for.

Since the interaction between aggregates is not considered, each inclusion (coarse aggregate) is assumed to experience the same stress field. The problem can be simplified as follows: first, the problem of an infinite plate with only one aggregate in it is investigated, focusing on the nucleation and growth of the interfacial crack under far field tensile stress. This solution is then generalized to the case of a body with multiple aggregates (and multiple but non-interacting interfacial cracks).

PRE-PEAK STRESS–STRAIN RELATION

Single aggregate problem

The problem of crack propagation in an elastic plate of unit thickness, containing one circular inclusion of radius R was solved by Cherepanov and reported by Zaitsev,[18] under the assumption expressed in Equation (1). The relation between the applied tensile load σ and the angle θ, which defines the crack size (see inset of Fig. 1), is given by the following equations:

$$\sigma = K_{Ic}^{if} F(\theta)/\sqrt{R}$$

$$F(\theta) = \frac{4(3 - \cos\theta)/\sqrt{\pi}}{\sqrt{\sin\theta\,(44 + 12\cos\theta + 12\cos^2\theta - 4\cos 4\theta + \sin^4\theta)}} \qquad (2)$$

where σ is the far field tensile stress and R is aggregate

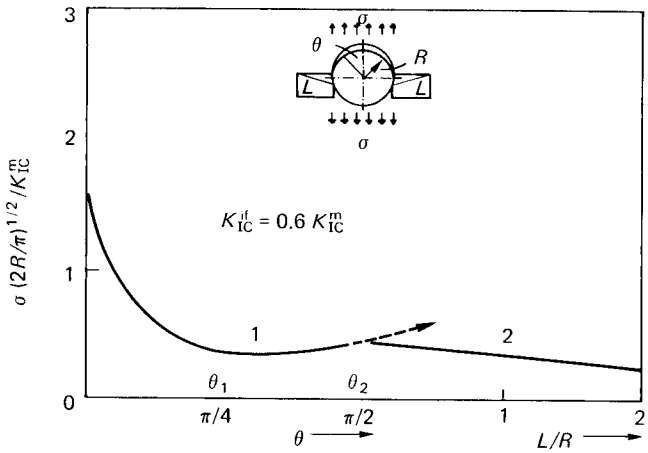

Fig. 1 Relation between normalized ambient uniaxial tensile stress and interfacial crack angle θ, from Ref. 19

radius. Line 1 in Fig. 1 shows this relationship; the y-axis gives values of the normalized load

$$\sigma^{o} = \left(\sigma\sqrt{2R/\pi}\right)/K_{Ic}^{m} \quad (3)$$

In the normalization, the value of K_{Ic}^{m} is taken as $K_{Ic}^{if}/0.6$ (consistent with the experimental results of Refs 23 and 24). (In the light of the mixed mode nature of interfacial crack propagation, and that the crack occurs at the interface of two dissimilar materials, a more rigorous analysis would prefer the use of interfacial fracture energy).

As the crack angle θ approaches zero, the stress reaches infinity. This phenomenon indicates that the stress required to initiate a crack from a perfect bonding is extremely large. In practice, however, the cracks probably initiate from flaw sites between the aggregate and matrix. For flaws with $\theta<\theta_1$ ($\theta_1 \approx \pi/4$), the crack propagates in an unstable manner (the descending part of line 1 in Fig. 1). This corresponds to a crack pop-in, and may be regarded as an interfacial crack nucleation process from an initial interfacial flaw. The crack can subsequently propagate in a stable manner until the applied load reaches a certain critical value, corresponding to the appearance of the crack branching into the matrix, illustrated in the inset of Fig. 1. The crack propagation within the matrix is an unstable process. Line 2 gives the value of the normalized stress *versus* the crack length for the crack propagation inside the matrix. This relationship is determined by approximating the interfacial and branch crack as a straight one with effective length $2(L + R)$, so that

$$\sigma\sqrt{\pi(L + R)} = K_{Ic}^{m} \quad (4)$$

where L is the length of crack in the cement matrix. The intersection of line 1 and line 2, labelled θ_2, indicates the moment when the crack at the cement/aggregate interface begins to branch into the matrix. For $K_{Ic}^{if}/K_{Ic}^{m} = 0.6$, $\theta_2 \approx \pi/2$.[18]

Multiple aggregates problem

To solve the multiple aggregates problem, the relation between the far field stress σ and the crack dimension θ at each cement/aggregate interface is assumed to be governed by the same curves shown in Fig. 1. According to Cherepanov's result, and if initial flaw sizes are similar at all aggregates, the interfacial cracks will first nucleate at the larger aggregates (Fig. 2). Nucleation at the largest aggregate interface is assumed to be associated with the point when the σ–ε curve deviates from a straight line. As σ increases, this interfacial crack continues to propagate stably around the interface, while other interfacial cracks nucleate and extend at other cement/aggregate interfaces. The enlargement of all interfacial cracks contributes to the inelastic deformation of the concrete.

A commonly used method for the calculation of the total strain of cracked solids is to superpose the two strain components, *ie*

$$\varepsilon = \varepsilon' + \varepsilon'' \quad (5)$$

where ε' is the elastic contribution of the unfractured material and ε'' is an additional inelastic component due to the opening of all interfacial cracks.

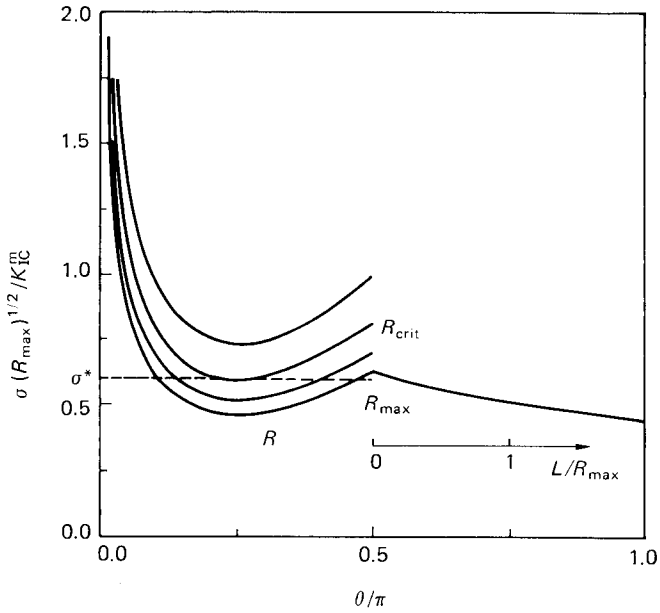

Fig. 2 Relation between normalized ambient uniaxial tensile stress and interfacial crack angle θ plotted for a family of aggregate sizes

The component ε' is simply equal to σ/E, where E is the Young's modulus of concrete without crack extension. The component ε'' can be found if it is assumed that the elongation caused by the displacement of the crack faces is 'smeared' over the volume of the sample. Thus, for a body containing n cracks

$$\varepsilon'' = \sum_{i=1}^{n} S_i/wh \quad (6)$$

where S_i is the opening area of crack i around the cement/aggregate interface, and w and h are the width and height of the uniaxially loaded specimen, respectively.

At a certain stress level σ, only some of the aggregates have cracks nucleated at their interfaces. These aggregates will have radii between a critical value R_{crit} and the maximum value R_{max}. R_{crit} is the radius of the smallest aggregate for which stable extension of the interfacial crack has begun and is therefore dependent on σ, Fig. 2. For continuous aggregate size distribution, the summation operation in Equation (6) may be replaced by an integration over R from R_{crit} to R_{max}

$$\varepsilon'' = \frac{1}{wh}\int_{R_{crit}}^{R_{max}} S(\sigma, R)\, p(R)\, dR \quad (7)$$

where $p(R)$ is the aggregate number density, *ie* $p(R)\,dR$ gives the number of aggregates with radii between R and $R+dR$.

An assumption has to be made for the distribution of aggregate size in the mixture. For this distribution, a Fuller curve is adopted. This curve results in a gradation of aggregate particles which leads to an optimum density and strength[26] and, therefore, is often used in concrete mix design. Other distributions are possible.

The Fuller distribution gives the relation

$$f(R) = \frac{1}{2\sqrt{RR_{max}}} \quad (8)$$

in which $f(R)\,dR$ is the percentage of total weight of aggregates with radii R to $R + dR$. The number density turns out to be

$$p(R) = \frac{V_{agg}}{2\pi\sqrt{R_{max}}} \times \frac{1}{R^2\sqrt{R}} \quad (9)$$

Substituting Equation (9) into (7), and using the ratio V_{agg}/wh as the volume fraction of aggregate in the 2-D case, represented by V_f, the total inelastic strain can be expressed as

$$\varepsilon'' = \frac{V_f}{2\pi\sqrt{R_{max}}} \int_{R_{crit}}^{R_{max}} S(\sigma, R) \frac{1}{R^2\sqrt{R}}\, dR \quad (10)$$

To calculate $S(\sigma,R)$, the opening area of a curved crack around the cement/aggregate interface, the opening area of a straight crack with the same length $2a$ as an approximation is used. Therefore, $a = R\theta$. The error induced by approximating the opening area of a curved crack by that of a straight one can be estimated, and is found to be negligible (within 6%).

For a straight crack with half length $a = R\theta$ under remote load σ

$$S \approx \frac{2\pi\sigma}{E}(1 - \nu^2)(R\theta)^2 \quad (11)$$

where ν is Poisson's ratio. Since the opening area contributing to the inelastic strain is the additional area after the interfacial crack pop-in, the opening area of the pre-existing bond crack, S_0, should be subtracted. S_0 is related to the properties of the pre-existing flaws at the cement/aggregate interfaces, such as the interface bonding and surface roughness. For simplicity, it is assumed that each of the inclusions has a bond crack of dimension $\theta_1 \approx \pi/4$, which corresponds to the beginning of the stable interfacial crack propagation stage. Therefore,

$$S = \frac{2\pi\sigma}{E}(1 - \nu^2) R^2 (\theta^2 - \theta_1^2) \quad (12)$$

Substituting Equation (12) into (10) gives

$$\varepsilon'' = \frac{V_f(1 - \nu^2)}{\sqrt{R_{max}}} \int_{R_{crit}}^{R_{max}} \frac{\sigma}{E} \frac{1}{\sqrt{R}} (\theta^2 - \theta_1^2)\, dR \quad (13)$$

For a given stress σ, either R or θ is used as the integration variable, since the crack dimension θ is related to the aggregate size by Equation (2). After integrating Equation (13) and adding the inelastic strain to the elastic strain, the total stress–strain relation is obtained

$$\frac{\sigma}{\sigma_{el}} = \frac{F(\theta)}{F(\theta_1)}$$

$$\frac{\varepsilon}{\varepsilon_{el}} = \frac{\sigma}{\sigma_{el}} \left\{1 + 2V_f \frac{(1 - \nu^2)}{F(\theta)} [(\theta^2 - \theta_1^2) F(\theta) - 2 \int_{\theta_1}^{\theta} \xi f(\xi)\, d\xi]\right\}$$

with $\frac{\sigma_{el}\sqrt{R_{max}}}{K_{Ic}^{if}} = F(\theta_1)$ and $\frac{\sigma\sqrt{R_{max}}}{K_{Ic}^{if}} = F(\theta)$ (14)

where θ varies from $\theta_1 \approx \pi/4$ to $\theta_2 \approx \pi/2$. In Equation (14) σ_{el} and ε_{el} are the stress and strain corresponding to the limit of proportionality, respectively.

The stress–strain curves predicted by the present model are plotted for indicated values of the aggregate volume fraction V_f in Fig. 3. With increasing aggregate volume fraction, the inelastic deformation of concrete increases, and the slope of the curve in the inelastic region gradually decreases. This phenomenon can be explained as follows: the inelastic deformation is associated with the deformation of interfacial cracks in the material. As more aggregates are put into the matrix, there will be an increase in the number of

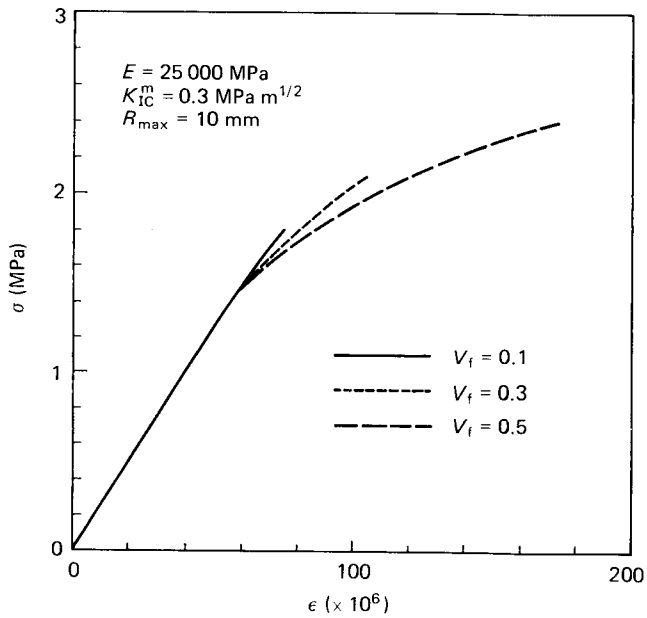

Fig. 3 The pre-peak stress–strain curve for different aggregate volume fractions, and for fixed R_{max}

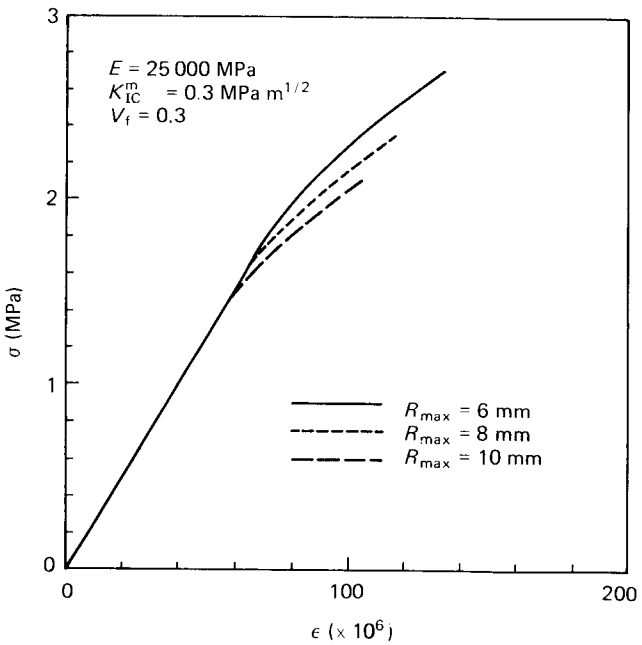

Fig. 4 The pre-peak stress–strain curve for different maximum aggregate sizes, and for fixed V_f

interfacial cracks, so that the material exhibits a stronger inelastic behaviour.

The effect of maximum aggregate size (for the same aggregate size distribution as defined in Equation (8)) on the degree of non-linearity of concrete is shown in Fig. 4. The result shows that using larger aggregates would lead to stronger nonlinear behaviour. Moreover, the deviation of the stress–strain curve from the linear stage occurs earlier.

Determination of tensile strength

Interfacial cracks can propagate stably until one of them starts to branch into the matrix. The crack propagation inside the matrix is unstable and is governed by line 2 in Fig. 1. It is generally accepted that the longest crack dominates the tensile failure of brittle materials. In the model, the peak load is predicted by assuming that the unstable propagation of one dominant crack leads to softening of the entire specimen. Because the branching of interfacial cracks into the matrix occurs first around the maximum-sized aggregate, with the largest initial interfacial crack (Fig. 2), it therefore becomes the dominant crack.

As the dominant crack expands into the matrix, it experiences the composite toughness due to the presence of all aggregates. The effective toughness of the composite, K_{Ic}^{eff}, is expected to be higher than that of the matrix because the dominant crack will deflect around the cement/aggregate interface as it intercepts an aggregate and the distributed interfacial cracks in front of the dominant crack will provide a shielding effect. Detailed development of the enhanced toughness due to distributed interfacial cracks as well as crack deflection is presented in Part II of this paper. For the present it is noted that K_{Ic}^{m} in Equation (4) has to be replaced by K_{Ic}^{eff}, so the tensile strength of the composite is given by

$$f_t = \frac{K_{Ic}^{eff}}{\sqrt{\pi R_{max}}} \tag{15}$$

$$K_{Ic}^{eff}/K_{Ic}^{m} = \sqrt{1.0 + 0.87\,V_f}\sqrt{\frac{1}{1 - (\pi^2/16)\,V_f\,(1 - \nu^2)}} \tag{16}$$

For $\nu = 0.20$, and $V_f = 0.1, 0.3, 0.5$ and 0.7, $K_{Ic}^{eff}/K_{Ic}^{m} = 1.07, 1.24, 1.43$ and 1.66, respectively.

Crack interactions

One of the basic assumptions made in the present model so far is that the interaction between interfacial cracks is negligible. This assumption can be justified only if the distances between interfacial cracks are large. For large aggregate volume fractions, the aggregates are packed closely and the interaction between interfacial cracks is expected to be strong, especially at the stage near the peak load. In the following, the effect of crack interaction on the peak load is investigated, resulting in a modified tensile strength.

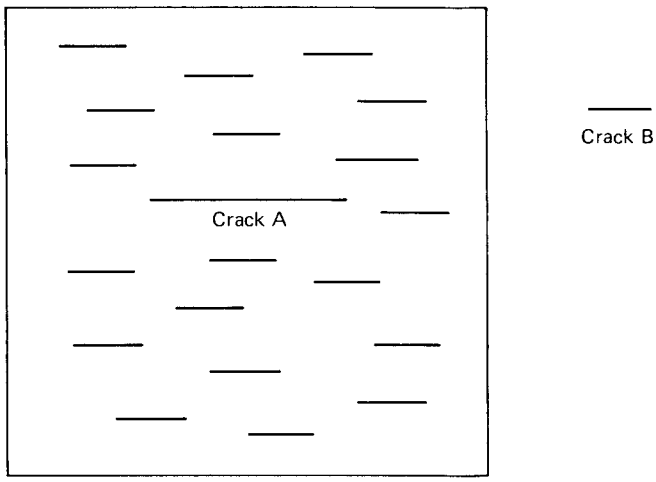

Fig. 5 A simplified model of crack interaction

Because the tensile strength is assumed to be controlled by branching of the largest interfacial crack into the matrix, the interaction of this largest crack with other cracks is being focused on. The interaction problem is simplified as a dominant straight crack of length $2R_{max}$ with all the other cracks of the average length $2R_{avg}$, as shown in Fig. 5. For the Fuller distribution

$$R_{avg} = \int_0^{R_{max}} Rf(R)\,dR = (1/3)R_{max} \tag{17}$$

The total stress intensity at the tip of the largest crack, K_{Ia}^{tot}, is the sum of two components

$$K_{Ia}^{tot} = K_{Ia}^{\infty} + K_{Ia}^{i} \tag{18}$$

where K_{Ia}^{∞} is the contribution from the applied load, and K_{Ia}^{i} is the additional contribution from the stress field induced by other cracks. Denoting the average additional stress at the crack A plane by σ_0, then,

$$K_{Ia}^{i} = \sigma_0\sqrt{\pi a} \tag{19}$$

The detail of the calculation of σ_0 is presented in the Appendix. Substituting Equation (19) into (18), the increase of the stress intensity at the tip of crack A is obtained:

$$K_{Ia}^{tot}/K_{Ia}^{\infty} = [1+f(a,b)]/[1-f(a,b)f(b,a)] \equiv \lambda \tag{20}$$

and

$$f(a,b) \equiv (1/2a)\left[\sqrt{(r+a)^2 - b^2} - \sqrt{(r-a)^2 - b^2} - 2a\right] \tag{21}$$

for (in the present case) $a = R_{max}$, $b = R_{avg}$ and $r =$

$$R_{max} + s + R_{avg} \tag{22}$$

where s is the average spacing (edge to edge) between aggregates. In the 2-D case, s is related to the aggregate volume fraction V_f (Fig. 6) by

$$V_f = \pi R_{avg}^2/l^2 \tag{23}$$

and

$$l = s + 2R_{avg} \tag{24}$$

Thus

$$s = \left(\sqrt{\frac{\pi}{V_f}} - 2\right) R_{avg} \tag{25}$$

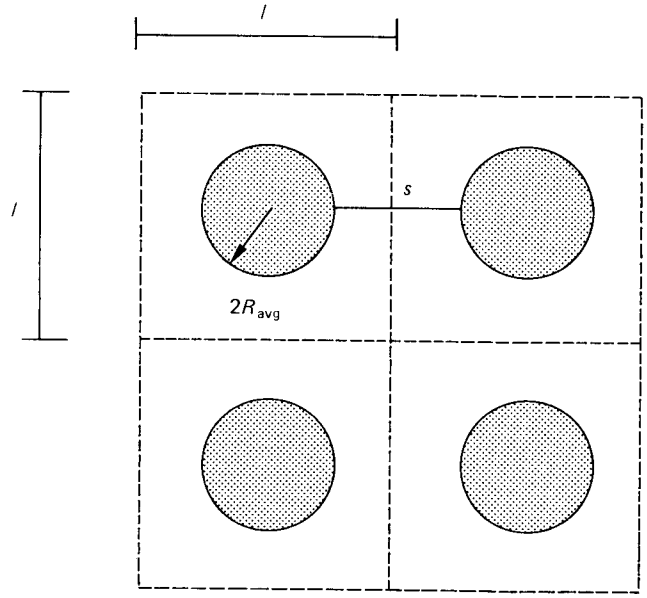

Fig. 6 A schematic diagram of the calculation of the average aggregate spacing

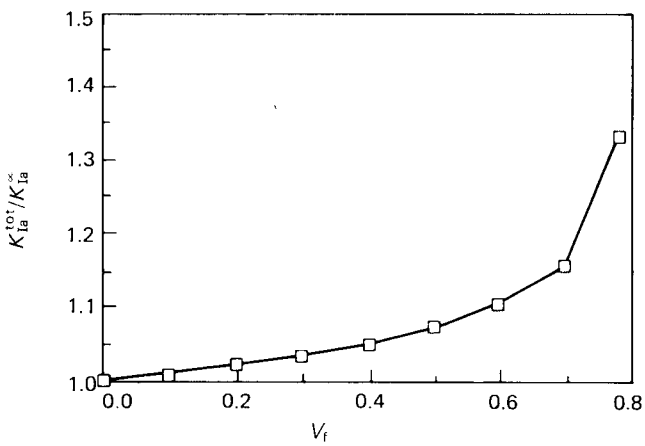

Fig. 7 The increase of stress intensity in the dominant crack tip due to crack interaction as a function of aggregate volume fractions

The increasing ratio of stress intensity at the largest crack tip, Equation (20), as a function of the aggregate volume fraction is plotted in Fig. 7. Generally, the interaction between interfacial cracks increases the stress intensity at the dominant crack tip, which is equivalent to a decrease in the material's toughness, K_{Ic}^{m}. Effectively, the material's loading capacity is reduced. Including the effect of crack interaction, the tensile strength in Equation (15) can be expressed as

$$f_t = \frac{\lambda K_{Ic}^{eff}}{\sqrt{\pi R_{max}}} \quad (26)$$

where λ (<1) is a function of V_f and was defined in Equation (20). The results indicate that the interaction effect is not substantial until $V_f = 0.4$. Therefore, the assumption of neglecting crack interactions at the pre-peak stage is acceptable for small aggregate volume fractions. For $V_f = 0.7$, however, the interaction decreases the peak load by approximately 16%.

It should be noted that there is an upper limit to the aggregate volume fraction, given by $V_f^0 = \pi/4 \approx 0.785$ for this method to work. Up to this limit, the value in the square root of the second term in Equation (21) becomes negative, which means that the interaction is so strong that the approach used in deriving Equation (20) breaks down.

Comparison of theoretical with experimental results

The effect of aggregate volume fraction on the properties of concrete has received relatively little attention as a specific research topic. Stock *et al*[29] reported a study of the influence of aggregate content on strength of concrete. The graded aggregate of 19 mm maximum size (diameter) was used. The comparison of results obtained here with the experimental data given by Ref. 29 is illustrated in Fig. 8. For aggregate volume fractions between 20 and 80%, both experimental and predicted results show an increasing trend in tensile strength. For V_f<20%, however, the experimental data shows a gradual decrease in strength, in contrast to the predicted results. Stock *et al* suggested that this decreasing trend may be associated with the uncertainty of the cement paste test results. On the other hand, the introduction of aggregates simultaneously introduces strength-limiting interfacial defects not present in the pure cement paste so that the experimental trend for V_f<20% could be real. This effect is not accounted for in the present modelling (which assumes a dominant crack emanating from a cement/aggregate interface for any V_f).

The effect of maximum aggregate size on tensile strength is plotted in Fig. 9, for a fixed aggregate volume fraction, $V_f = 0.7$. The presence of coarse aggregates generally reduces strength. If the maximum aggregate size is larger than 5 mm, the model predicts the tensile strength to be equal to 1.5–3.5 MPa, which is very close to the typical value of concrete tensile strength given in the literature.[27,28] As aggregate size becomes smaller and smaller, however, the predicted tensile strength reaches infinity. This result is due to the limitation of the model, in which the microcrack size in the matrix is assumed to be negligible compared with the interfacial crack lengths. However, when the aggregate size reduces to a very small value, matrix

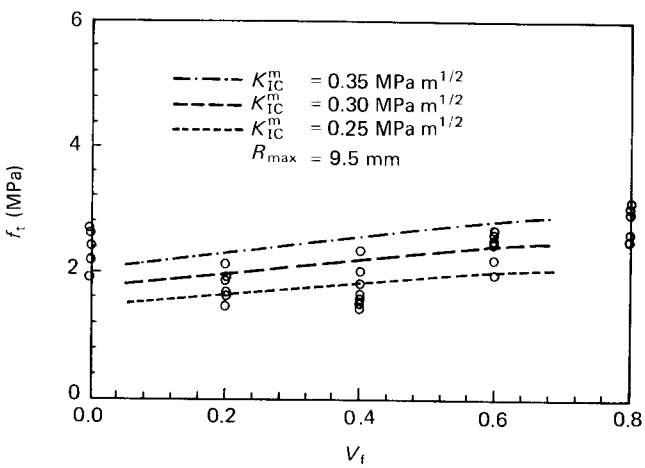

Fig. 8 Comparison of model predicted and measured relation between tensile strength and aggregate volume fraction. The experimental data is from Ref. 29

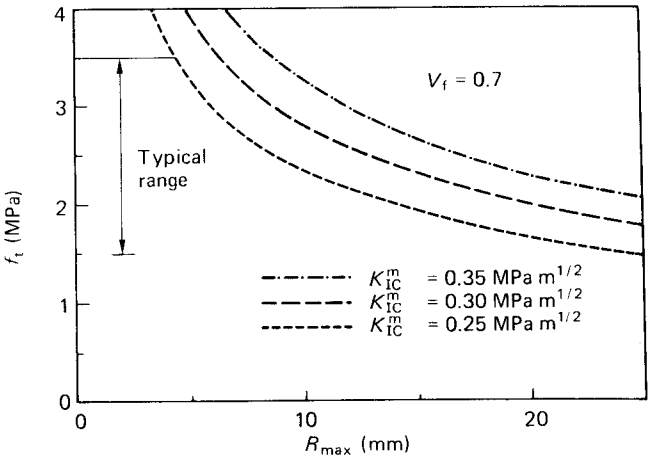

Fig. 9 Dependency of model predicted tensile strength on maximum aggregate size and typical range of f_t for normal concrete

crack propagation may be expected to dominate over interfacial crack propagation. The upper horizontal line in Fig. 9 indicates the tensile strength of the mortar matrix, which sets the upper limit of conventional concrete tensile strength. The combination of these two curves represents a complete relationship between tensile strength f_t and maximum aggregate size R_{max}.

Results of investigations concerning the influence of maximum aggregate/sand size on the concrete/mortar tensile strength have been reported.[6,8,31,32,33] Kaplan[6,31] observed that the presence of coarse aggregate generally reduces the flexural strength of concrete to below that of mortar. Hughes and Chapman[8] reported a decrease of tensile strength with increasing maximum aggregate size in a uniaxial tensile test, especially for round shaped aggregate. However, contradictory experimental results can also be found. Wolinski *et al*[32] concluded from the test results that there is no monotonic influence of aggregate particle size on fracture mechanics parameters, including the tensile strength.

The predicted stress–strain relations are compared with the experimental data [9] in Fig. 10(a). The maximum aggregate size is not reported so a typical value is used in the calculation. The cement matrix toughness K_{Ic}^m, also not given, has assumed values extrapolated from data given by Ref. 30, Fig. 11, where K_{Ic}^m was measured as a function of the water/cement ratio. For a water/cement ratio=0.45 and 0.60, K_{Ic}^m = 0.32 and 0.24, respectively. The generated curves seem to underestimate the inelastic deformation. Using slightly smaller K_{Ic}^m values (but still in the reasonable range) provides a good agreement between the model prediction and experimental stress–strain measurements, as shown in Fig. 10(b).

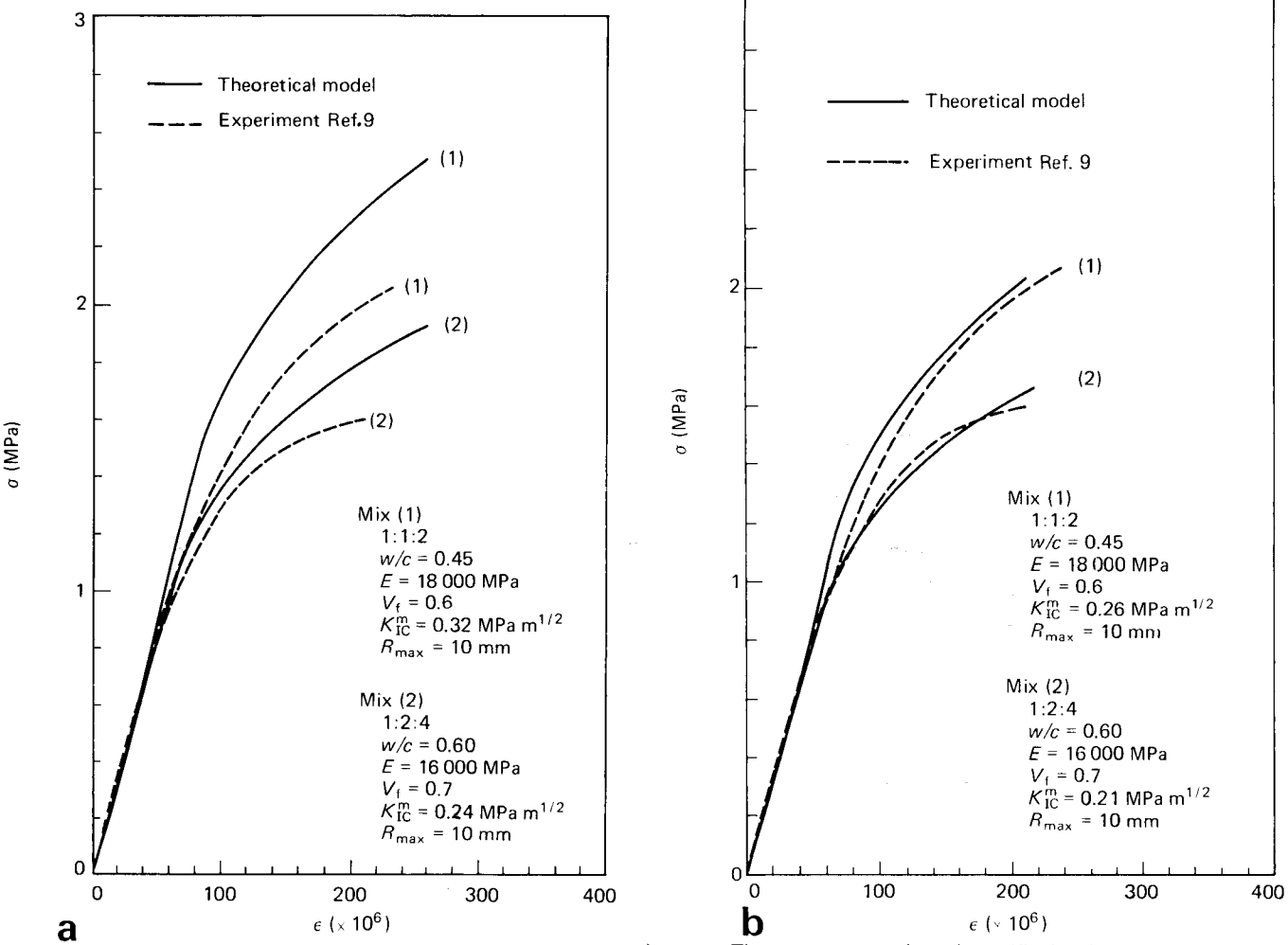

Fig. 10 Comparison of model predicted and measured stress–strain curve. The aggregate and sand specific density is assumed to be 2.6, and cement specific density 3.15, approximately, in the calculation of V_f. The experimental data is from Ref. 9

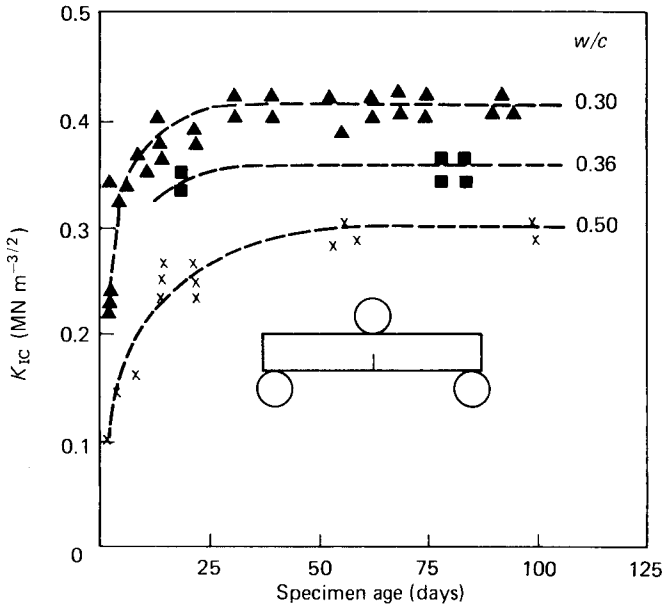

Fig. 11 Experimental measurements of cement matrix toughness K_{IC}^{m} *versus* water/cement ratio, given by Ref. 30

CONCLUSIONS

A simple theoretical model of the tensile behaviour of concrete in the pre-peak stage was established, considering concrete as a composite of two phases, cement matrix and aggregates. The model relates the internal structures and local deformation mechanisms to the macroscopic tensile behaviour of concrete. The effects of maximum aggregate size, aggregate volume fraction and cement matrix toughness on the degree of inelastic deformation as well as the tensile strength are analysed. The amount of inelastic deformation prior to peak load increases with V_f and R_{max}. The tensile strength increases with increasing V_f for fixed R_{max}, and with decreasing R_{max}, for fixed V_f. The predicted stress–strain relation compares reasonably well with limited experimental data. However, it should be emphasized that contradictory experimental results can be found. Apart from the model simplifications already pointed out, it may be expected that the 3-D nature of internal structure and deformation mechanisms, and the irregular geometry of the aggregates must have an effect on the composite tensile behaviour.

ACKNOWLEDGEMENTS

The authors would like to thank A. Hillerborg and S. Mindess for many helpful discussions. A grant from the National Science Foundation to the Massachusetts Institute of Technology is gratefully acknowledged.

REFERENCES

1 **Slate, F. O. and Hover, K. C.** 'Microcracking in concrete' in '*Fracture Mechanics of Concrete*' (eds A. Carpinteri and A. R. Ingraffea) (1984) pp 137–159
2 **Slate, F. O. and Matheus, R. F.** 'Volume changes on setting and curing of cement paste and concrete from zero to seven days' *J Amer Concr Inst Proc* **64** (1967) pp 34–39
3 **Hsu, T. T. C. and Slate, F. O.** 'Tensile bond between aggregate and cement paste or mortar' *J Amer Concr Inst Proc* **60** (1963) pp 465–486
4 **Shah, S. P. and Slate, F. O.** 'Internal microcracking, mortar-aggregate bond and the stress–strain curve of concrete' *Cement and Concrete Ass London* (1968) pp 82–92
5 **Todd, J. D.** 'The determination of tensile stress/strain curves for concrete' *Proc Inst Civil Engrs* **4** 2 Part I (1955) pp 201–211
6 **Kaplan, M. F.** 'Flexural and compressive strength of concrete as affected by the properties of coarse aggregates' *J. Amer Concr Inst* **55** (1959) pp 1193–1208
7 **Kaplan, M. F.** 'Strains and stresses of concrete at initiation of cracking and near failure' *Proc J Amer Concr Inst* **60** (1963) pp 853–880
8 **Hughes, B. P. and Chapman, G. P.** 'The complete stress strain curves for concrete in direct tension' *RILEM Bull* **30** (1966) pp 95–97
9 **Evans, R. H. and Marathe, M. S.** 'Microcracking and stress–strain curves for concrete in tension' *Materiaux et Constructions* **1** (1968) pp 61–64
10 **Zielinski, A. J.** 'Behavior of concrete at high rates of tensile loading: A theoretical and experimental approach' *Report 5-83-5 Stevin Lab* (Delft University of Technology)
11 **Lorrain, M. and Loland, K. E.** 'Damage theory applied to concrete' in '*Fracture Mechanics of Concrete*' (ed F. H. Wittmann) (1983) pp 341–369
12 **Mazars, J.** 'Mechanical damage and fracture of concrete structures' *5th Int Conf on Fracture (1980), Cannes, France*
13 **Mihashi, H.** 'A stochastic theory for fracture of concrete' in '*Fracture Mechanics of Concrete*' (ed F. H. Wittmann) (1983) pp 301–339
14 **Hu, X. Z., Cotterell, B. and Mai, Y. W.** 'A statistical theory of fracture in a two-phase brittle material' *Proc Roy Soc London* **A401** (1985) pp 251–265
15 **Ortiz, M.** 'A constitutive theory for the inelastic behavior of concrete' *Mech Mater* **4** (1985) pp 67–93
16 **Hu, X. Z., Cotterell, B. and Mai, Y. W.** '*Computer simulation models of fracture in concrete*' (Elsevier Science Publishers B.V. Amsterdam, The Netherlands 1986)
17 **Weibull, W.** *Proceedings of the Royal Swedish Institute of Engineering Research* **151** (1939) pp 151
18 **Zaitsev, Yu. V.** 'Inelastic properties of solids with random cracks' in '*Mechanics of Geomaterials*' (ed Z. Bazant) (1985) pp 89–128
19 **Zaitsev, Y.** 'Crack propagation in a composite material' in '*Fracture Mechanics of Concrete*' (ed F. H. Wittmann) (1983) pp 251–299
20 **Mindess, S. and Diamond, S.** 'The cracking and fracture of mortar' *Materiaux et Constructions* **15** (1982) pp 107–113
21 **Mindess, S. and Diamond, S.** 'A device for observation of cracking of cement paste or mortar under compressive loading within a scanning electron microscope' *Cem Concr Res* **12** (1982) pp 569–576
22 **Maji, A. K. and Shah, S. P.** 'A study of fracture process of concrete using acoustic emission' *Proc Soc Expt Mech Spring Conference* (June 1986)
23 **Hillemeier, B. and Hilsdorf, H. K.** 'Fracture mechanics studies on concrete compounds' *Cem Concr Res* **7** (1977) pp 523–536
24 **Ziegeldorf, S.** 'Fracture mechanics parameters of hardened cement paste, aggregates and interfaces' in '*Fracture Mechanics of Concrete*' (ed F. H. Wittmann) (1983) pp 371–409
25 **Liu, T. C. Y., Nilson, A. H. and Slate, F. O.** 'Stress–strain response and fracture of concrete in uniaxial and biaxial compression' *J Amer Concr Inst Proc* **69** (1972) pp 291–295
26 **Mindess, S. and Young, J. F.** '*Concrete*' (Prentice-Hall Inc, 1981)
27 **Neville, A. M.** '*Properties of Concrete*' (Pitman, 1981)
28 **Illston, J. M. *et al*** '*Concrete, Timber and Metals*' (Van Nostrand Reinhold, 1979)
29 **Stock, A. F. D., Hannant, J. and Williams, R. I. T.** 'The effect of aggregate concentration upon the strength and modulus of elasticity of concrete' *Mag Concr Res* **31** 109 (1979) pp 225–234
30 **Higgins, D. D. and Bailey, J. E.** 'Fracture measurements on cement paste' *J Mater Sci* **11** (1976) pp 1995–2003
31 **Jones, R. J. and Kaplan, M. F.** 'The effect of coarse aggregate on the mode of failure of concrete in compression and flexure' *Magazine of Concr Res* **9** 26 (1957) pp 89–94
32 **Wolinski, S., Hordijk, D. A., Reinhardt, H. W. and Cornelissen, H. A. W.** 'Influence of aggregate size on fracture mechanics parameters of concrete' *Int J Cement Composites Lightweight Concr* **9** 2 (1987) pp 95–103
33 **Swift, D. S., Nicholas, D. M. and Scott, R. A. M.** 'The effect of sand particle size on the tensile strength of cement mortars' *Int J Cement Composites Lightweight Concr* **8** 1 (1986) pp 39–44

AUTHORS

The authors are with the Department of Civil Engineering, Massachusetts Institute of Technology, Cambridge, MA 02139, USA.

APPENDIX. Calculation of crack interactions

Consider first an isolated crack of length $2a$ (crack A) in an infinite medium under ambient tensile stress σ^∞. The stress intensity at the tip of this crack simply takes the form

$$K_{Ia}^{\infty} = \sigma^{\infty}\sqrt{\pi a} \tag{A1}$$

Now consider the interaction between cracks. Adding one more crack of length $2b$ (crack B) into the body would generate an additional elastic field, which gives an additional contribution, K_{Ia}^{i}, at the tip of crack A, *ie*

$$K_{Ia}^{tot} = K_{Ia}^{\infty} + K_{Ia}^{i} \tag{A2}$$

where K_{Ia}^{tot} is the total stress intensity at the tip of crack A. Crack A now experiences a K_{Ia}^{∞} from the applied stress and a K_{Ia}^{i} from the induced field of crack B. Its magnitude is

$$K_{Ia}^{i} = \sigma_0\sqrt{\pi a} \tag{A3}$$

where σ_0 is the additional stress induced by crack B. The value of σ_0 remains to be evaluated. It obviously varies with the position of crack A with respect to crack B. For simplicity, the worst case where crack A and B are colinear is considered. Thus, the stress distribution in the crack A plane is

$$\sigma_0(x) = \frac{K_{Ib}^{\infty}}{\sqrt{\pi b}}\left(\frac{x}{\sqrt{x^2 - b^2}} - 1\right) \tag{A4}$$

where

$$K_{Ib}^{\infty} = \sigma^{\infty}\sqrt{\pi b} \tag{A5}$$

and x is the horizontal distance measured from the centre of crack B.

Averaging $\sigma_0(x)$ over crack A yields

$$\sigma_0 = \frac{K_{Ib}^{\infty}}{\sqrt{\pi b}} f(a, b) \tag{A6}$$

where r is the distance between the centres of two cracks and

$$f(a, b) \equiv \frac{1}{2a}\left[\sqrt{(r + a)^2 - b^2} - \sqrt{(r - a)^2 - b^2} - 2a\right] \tag{A7}$$

Substituting Equations (A7), (A6) and (A3) into (A2) gives

$$K_{Ia}^{tot} = K_{Ia}^{\infty} + K_{Ib}^{\infty} f(a, b)\sqrt{(a/b)} \tag{A8}$$

Notice that crack B also experiences the elastic field induced by crack A. Hence, K_{Ib}^{∞} in Equation (A8) should be replaced by K_{Ib}^{tot}. Equation (A8) thus becomes

$$K_{Ia}^{tot} = K_{Ia}^{\infty} + K_{Ib}^{tot} f(a, b)\sqrt{(a/b)} \tag{A9}$$

Similarly, the same method can be applied to crack B and a similar equation results

$$K_{Ib}^{tot} = K_{Ib}^{\infty} + K_{Ia}^{tot} f(b, a)\sqrt{(b/a)} \tag{A10}$$

Solving Equations (A9) and (A10) simultaneously for two unknowns, K_{Ia}^{tot} and K_{Ib}^{tot} gives

$$\frac{K_{Ia}^{tot}}{K_{Ia}^{\infty}} = \frac{1 + f(a, b)}{1 - f(a, b)f(b, a)} \tag{A11}$$

or

$$K_{Ia}^{tot} = K_{Ia}^{\infty}\left\{1 + \frac{f(a, b)[1 + f(b, a)]}{1 - f(a, b)f(b, a)}\right\} \tag{A12}$$

The second term inside the brackets describes the interaction.